

Information scrambling and chaos induced by a Hermitian Matrix

Sven Gnutzmann¹ and Uzy Smilansky²

¹*School of Mathematical Sciences, University of Nottingham, United Kingdom and*

²*Department of Physics of Complex Systems, The Weizmann Institute, Rehovot, Israel*

Given an arbitrary $V \times V$ Hermitian matrix, considered as a finite discrete quantum Hamiltonian, we use methods from graph and ergodic theories to construct a *quantum Poincaré map* at energy E and a corresponding stochastic *classical Poincaré-Markov map* at the same energy on an appropriate discrete *phase space*. This phase space consists of the directed edges of a graph with V vertices that are in one-to-one correspondence with the non-vanishing off-diagonal elements of H . The correspondence between quantum Poincaré map and classical Poincaré-Markov map is an alternative to the standard quantum-classical correspondence based on a classical limit $\hbar \rightarrow 0$. Most importantly it can be constructed where no such limit exists. Using standard methods from ergodic theory we then proceed to define an expression for the *Lyapunov exponent* $\Lambda(E)$ of the classical map. It measures the rate of loss of classical information in the dynamics and relates it to the separation of stochastic *classical trajectories* in the phase space. We suggest that loss of information in the underlying classical dynamics is an indicator for quantum information scrambling.

I. INTRODUCTION

Quantum information scrambling and operator growth is currently investigated in many fields such as black holes theory [1–4], condensed matter many-body physics [5], and quantum information theory [6]. They brought together developments in quantum information and quantum chaos, and sparked a large overarching interest that also lead to experimental observations [7–9]. Mathematically, quantum information scrambling is related to seminal results such as the Lieb-Robinson (LR) quantum speed limits [10, 11]. One of the main tools used to quantify information scrambling is the so-called out-of-time-ordered commutators [OTOC], initially introduced in condensed matter physics [12] (see [13] for an overview and further references). The exponential growth of OTOC is assumed to signal operator growth and information scrambling.

In classical mechanics, information scrambling is associated with classical chaos. In contrast with its quantum counterpart, it is a well defined concept where both physical and mathematical tools and methods are available to study and quantify chaotic loss of information [14, 15]. They provide a solid explanation why deterministic mechanical systems might not be predictable which justifies their study using statistical rather than deterministic methods.

No wonder therefore that the quantum correspondence principle was tried to link the study of quantum chaotic features with an underlying classical concepts. Indeed, in [3, 4] the exponential growth rate of OTOC was suggested as the ‘quantum butterfly effect’ and ‘quantum Lyapunov exponent’. However, this notion is rather limited since exponential growth of OTOCs has been found even in classically regular systems [16, 17]. The study of quantum systems which are defined by quantizing classical chaotic systems was the subject of the field of quantum chaos [14, 18, 19]. The main tool was the study of the quantum systems in the limit $\hbar \rightarrow 0$. Clearly, not all the classical quantities could be transplanted to the quantum theory. Yet, one could still ask what are the finger-prints of classical chaos in the quantum description. The BGS conjecture [20] e.g., suggests that the spectral statistics of ‘typical’ classically chaotic quantum systems follow the statistics provided by Random Matrix Theory (RMT). This conjecture does not apply in the other direction – namely, a quantum system may display RMT statistics without having a chaotic classical counterpart. As an example consider two different random matrix ensembles: The Wigner-Dyson ensembles where all the matrix elements are randomly distributed, and the Dumitriu-Edelman ensembles ($G\beta E$) [21] with random entries forming tridiagonal matrices. They share precisely the same spectral distribution functions. However, while eigenvectors of the former are uniformly distributed (an indicator for chaos via the Shnirelman theorem [22]), those of the latter display a transition from localised eigenfunctions (implying suppressed chaos) for $\beta \leq 2$ values to extended eigenfunctions otherwise [23]. We will return to this example in the sequel. In general, a single quantum signature of chaos – such as spectral statistics – as indicator might lead to an incomplete or insufficient picture of the chaoticity of the quantum system.

The purpose of this note is to introduce a new method for quantifying the degree of information loss (or chaoticity) induced by quantum evolution. Being the first time this approach is presented, its ideas and main results will be explained, leaving applications and further results to later publication.

The system to be discussed is driven by a quantum Hamiltonian represented as a finite matrix. The quantum evolution reduces in the semi-classical limit to a discrete stochastic classical dynamics expressed in terms of a Poincaré-Markov map. Ergodic theory is then used to define a classical Lyapunov exponent. It describes the flow and loss of information in the classical dynamics and relates it to the deviation of (stochastic) trajectories in a discrete phase

space which is constructed specifically for the Hermitian matrix of interest.

The new approach builds upon ideas, results and methods from spectral graph theory and ergodic theory. It uses the results of a recent work which provides an energy dependent unitary map $U(E)$ – to which we refer as the *Quantum Poincaré map* – to a Hermitian matrix H in a non-trivial way such that an underlying graph structure is obeyed [24, 25]. This Quantum Poincaré map acts on an associated phase space – and the classical dynamics is obtained by replacing quantum transition amplitudes by their absolute squares. We call this the Poincaré-Markov map as it is a stochastic matrix that generates a Markov process. A similar quantum-classical correspondence was introduced [26, 27] for quantum graphs, (see [28] and references therein). It was used e.g., to set criteria to determine which graphs would display RMT spectral statistics [26–33].

A few examples show how the classical Lyapunov exponent reflects localization properties of wave functions. Further applications and results as well as future research directions, together with a discussion of the relation to OTOC and the LR speed limit [10, 11] are deferred to the last section.

II. THE CLASSICAL DYNAMICS ASSOCIATED WITH A MATRIX AND THE LYAPUNOV EXPONENT

The quantum system under study is governed by a Hamiltonian which is represented as a $V \times V$ Hermitian matrix H_{vw} with D non-vanishing off-diagonal elements. Without loss of generality it is assumed that H is not block-diagonal. The energy spectrum and eigenvectors satisfy,

$$\sum_{w=1}^V H_{vw} \phi_w = E \phi_v \quad (1)$$

The theory is presented below in the following steps:

- Step 1** Eq. (1) is rewritten as a discrete Schrödinger equation with “kinetic energy” and “local potential” terms on a graph with V vertices and D directed edges. The set of vertices is naturally defined as the *configuration-space* on the graph. The analogous classical dynamics is that of hopping between neighbouring vertices.
- Step 2** A discrete momentum on the graph is introduced so that the classical *phase-space* is the set of directed edges on the graph. The quantum evolution operator or *Quantum Poincaré map* is expressed as a $D \times D$ unitary matrix $U(E)$ in the directed-edge basis. The intimate connection between H and $U(E)$ is evident since the spectrum of H consists of the zeros of $\det(\mathbb{I}_D - U(E))$.
- Step 3** The corresponding classical dynamic – the *Poincaré-Markov* map – is expressed in terms of classical transition *probabilities*. They are defined as the absolute squares of the quantum transition *amplitudes* which are the matrix elements of $U(E)$. The matrix obtained this way is a bi-stochastic matrix which defines a Markovian evolution on the graph.
- Step 4** Finally, standard methods from ergodic theory are used to compute the Lyapunov exponent and its variance for the Poincaré-Markov map associated to (1) at a given energy E .

Many of the ideas and methods applied in this work were discussed and used in other contexts. We harness them here in order to introduce the novel approach to information scrambling and chaoticity which is to be unfolded.

Step 1: A discrete Schrödinger operator on an underlying graphs

We associate to the matrix H an underlying graph \mathcal{G} with V vertices and adjacency matrix

$$A_{vw} = \begin{cases} 1 & \text{if } H_{vw} \neq 0 \text{ and } v \neq w, \\ 0 & \text{else.} \end{cases} \quad (2)$$

The degree of a vertex v is denoted by $d_v = \sum_{w=1}^V A_{vw}$. The graph vertex set \mathcal{V} forms the *configuration space*. The Hamiltonian H can be written as a generalised tight-binding Schrödinger operator $H = -L + W$ with a kinetic energy (Laplacian) part $-L$ that describes the hopping and a diagonal potential W

$$L_{vw} = \Gamma_v \delta_{vw} - H_{vw}(1 - \delta_{vw}) \quad \text{and} \quad W_{vw} = (H_{vv} + \Gamma_v) \delta_{vw}.$$

Here, $\Gamma_v = \sum_{u \neq v} |H_{vu}|$ is known as *Gershgorin parameter* [34]. It will appear often in the sequel. The Gershgorin circle theorem [34] implies that $-L$ is a non-negative matrix. If $H = -A$ the Gershgorin parameters reduce to $\Gamma_v = d_v$

and L to the standard combinatorial graph Laplacian [24, 25]. Classical trajectories in configuration space are strings of connected vertices.

Step 2: The phase space and definition of the unitary quantum map

To define the corresponding *phase space*, recall that in classical mechanics the momentum points from the present point in configuration space to its future position. *A-priori*, any vertex u could be the “next” vertex to the starting vertex v . However, the graph connectivity limits the possible choices to the adjacent vertices where $A_{uv} = 1$. It is natural to define the *momentum space* as the vertex set which can be reached from a given vertex by a single hopping. Thus, A defines the domain of allowed momenta. A directed pair of connected vertices forms a directed edge. Thus, *Phase space* is the space of all directed edges. Their total number is $D = \sum_{v,w=1}^V A_{vw}$. For a given directed edge $e = (vw)$, the *origin* is $w = o(e)$ and the *terminus* is $v = \tau(e)$. Classical trajectories in phase space are strings of connected directed edges e_i where $o(e_{i+1}) = \tau(e_i)$.

The *phase space* evolution will now be expressed in terms of a unitary evolution operator on a D dimensional space of amplitudes a_{vw} with $(vw) \in \mathcal{D}$. On a given edge that connects v and w the amplitudes a_{vw} and a_{wv} are defined in terms of the vertex amplitudes ϕ_v , ϕ_w of (1). It is convenient to denote $H_{vw} = h_{vw}e^{2i\gamma_{vw}}$ with $h_{vw} = |H_{vw}|$ and $\gamma_{vw} \in (-\frac{\pi}{2}, \frac{\pi}{2}]$. Then,

$$\phi_w = \frac{e^{i\gamma_{vw}}}{\sqrt{h_{vw}}} \left[a_{wv}e^{-i\pi/4} + a_{vw}e^{i\pi/4} \right] \quad \text{and} \quad \phi_v = \frac{e^{i\gamma_{vw}}}{\sqrt{h_{vw}}} \left[a_{wv}e^{i\pi/4} + a_{vw}e^{-i\pi/4} \right]. \quad (3)$$

Consider a vertex v with degree d_v and the vertices $\{w\}$ which are connected to it. There are $2d_v$ directed edges with $o(e) = v$ (outgoing) or $\tau(e) = v$ (incoming). The corresponding set of a_e must all satisfy (3) on all edges connected to v . This requirement offers $d_v - 1$ independent homogeneous linear equations which the set of a_e must satisfy. One further homogeneous linear equation follows directly from (1) by considering the v -th row which involves ϕ_v and all the connected ϕ_w . Thus the set of $2d_v$ amplitudes must satisfy d_v equations – which provide a linear relation between the set of all outgoing amplitudes a_{vw} and the set of all incoming amplitudes a_{wv} :

$$\mathbf{a}^{(out)} = \sigma^{(v)}(E)\mathbf{a}^{(in)} \quad \text{where} \quad \sigma_{w'w}^{(v)}(E) = i\delta_{w'w} - 2\frac{\sqrt{h_{vw'}h_{vw}}}{H_{vw} - E - i\Gamma_v} e^{i(\gamma_{vw'} + \gamma_{wv})}. \quad (4)$$

The matrix $\sigma^{(v)}(E)$ is a $d_v \times d_v$ unitary matrix for any real E . It depends on the matrix-elements of the v row in H . Combining all the vertex conditions (4) to a single D dimensional matrix and observing the rule that a directed edge (wv) plays a double role – incoming (to w from v) and outgoing (from v to w) – one finds that the D dimensional amplitude vector must satisfy $\mathbf{a} = U(E)\mathbf{a}$. Hence $\det[\mathbb{I} - U(E)] = 0$ is satisfied if and only if E is in the spectrum of H . The Quantum Poincaré map $U(E)$ is a unitary matrix defined by

$$U_{v'w',vw}(E) = \delta_{w'v}\sigma_{v'w}^{(v)}(E) \quad \text{or} \quad U(\lambda) = P\Sigma(E), \quad (5)$$

where P is a permutation matrix and $\Sigma(E)$ is a block diagonal matrix with the V diagonal blocks $\sigma^{(v)}(E)$. $U(E)$ is unitary for any real E . The determinant identity

$$\zeta_H(E) \equiv \det[\mathbb{I} - U(E)] = \frac{2^E \det[E - H]}{\prod_{v=1}^V (H_{vv} - E - i\Gamma_v)}. \quad (6)$$

proves that the real zeros of $\zeta_H(E)$ coincide with the spectrum of H and its poles lie in the lower half of the complex plane [24, 25].

Step 3: Construction of the discrete classical dynamics

The matrix elements of the Quantum Poincaré map $U(E)$ are the transition amplitudes for the discrete step. The absolute squares

$$B_{e',e}(E) = |U_{e',e}(E)|^2 \quad (7)$$

are transition probabilities which define an analogue classical dynamics in terms of a Markov process on the underlying phase space of directed edges. We refer to this as the Poincaré-Markov map. The classical probabilities $p_e^{cl}(n)$ to be on the directed edge e after n time steps evolve by

$$p_{e'}^{cl}(n+1) = \sum_{e \in \mathcal{D}} B_{e',e}(E) p_e^{cl}(n). \quad (8)$$

This ‘Liouvillian dynamics’ is the natural classical counterpart of the quantum mechanical description induced by the quantum map $U(E)$. The trajectories which contribute to the transition $e \rightarrow e'$ in n steps are the same for both the classical and quantum descriptions. However the quantum interference obtained by summing *amplitudes* is replaced in the classical expression by summing transition *probabilities*. Comment : The matrix elements of $B(E)$ do not depend on the phases of H_{uv} when $u \neq v$. This could be overcome partially by constructing the stochastic matrix from elements of $(U^2)_{uv}$ [38].

The matrix $B(E)$ is bi-stochastic $\sum_{e \in \mathcal{D}} B(E)_{ee'} = 1 = \sum_{e' \in \mathcal{D}} B(E)_{ee'}$. Bi-stochastic matrices that are obtained from a unitary matrix in an analogue way have been called *uni-stochastic* and have been discussed in detail for quantum graphs [30–32] where an analogous quantum-classical correspondence has been used very effectively to understand quantum chaos (see [25] and references therein).

As such $B(E)$ has the following properties: Its spectrum, denoted by $\{\nu_j\}_{j=1}^D$ is restricted to the unit disc in the complex plane, complex eigenvalues appear in conjugate pairs. The uniform distribution $|\nu_1\rangle = \frac{1}{\sqrt{D}}(1, 1, \dots, 1)^T$ is invariant, that is, it is an eigenvector with eigenvalue $\nu_1 = 1$. This is known as the Frobenius eigenvalue and eigenvector and we reserve the index 1. When all eigenvalues but ν_1 are strictly inside a disc of radius 1 the evolution is mixing and the dynamics decays to the uniform distribution exponentially fast.

Many properties of the system can be computed in terms of the matrix $B(E)$ and its spectrum. E.g. the rate of entropy production and the probability to return to the starting position after a given time. We focus on measures of chaoticity as expressed in terms of the Lyapunov exponents.

Step 4: The Lyapunov Exponent

In the present context a trajectory is just a sequence of connected edges:

$$\xi = \{(e_t)_{t=-\infty}^{\infty} : e_t \in \mathcal{D}, t \in \mathbb{Z}, \tau(e_t) = o(e_{t+1})\} . \quad (9)$$

It can be considered as a string picked up from a collection of D letters. The propagation along the itinerary is described by the *shift operation* $e_t \mapsto e_{t+1}$. Systems with trajectories which follow the above definitions are called *shifts of finite type* and are abundantly studied in ergodic theory [29, 35–37].

Consider a finite section of a trajectory: $\xi_t = (e_j)_{j=0}^t$ which start at a prescribed directed edge e_0 . The probability that this trajectory will be traversed in the stochastic evolution induced by $B(E)$ is

$$P(\xi_t) = \prod_{j=1}^t B_{e_j, e_{j-1}} . \quad (10)$$

The mean Lyapunov exponent is defined as

$$\langle \Lambda(E) \rangle = - \lim_{nt \rightarrow \infty} \frac{1}{t} \langle \log[P(\xi_t)] \rangle_{\xi_t} \quad (11)$$

where the average is over all trajectories of length t and all initial e_0 .

The thermodynamic formalism provides powerful methods to compute the Lyapunov exponent. This is done by introducing an auxiliary $D \times D$ matrix

$$Q_{e, e'}(\beta) = [B(E)_{e, e'}]^\beta, \quad \beta \geq 0 . \quad (12)$$

Denoting the eigenvalue of $Q_{e, e'}(1 + \epsilon)$ with the largest real part by $\mu(\epsilon)$, one finds

$$\langle \Lambda(E) \rangle = - \left. \frac{\partial \log[\mu(\epsilon)]}{\partial \epsilon} \right|_{\epsilon=0}, \quad \text{and} \quad \langle \Lambda(E)^2 \rangle - \langle \Lambda(E) \rangle^2 = \left. \frac{\partial^2 \log[\mu(\epsilon)]}{\partial \epsilon^2} \right|_{\epsilon=0} . \quad (13)$$

A simple computation shows

$$\langle \Lambda(E) \rangle = - \frac{1}{D} \sum_{e, e' \in \mathcal{D}} B(E)_{e, e'} \log B(E)_{e, e'} . \quad (14)$$

The expression for the second moment is quoted here for the sake of completeness

$$\langle \Lambda^2(E) \rangle = \frac{1}{D} \sum_{e, e' \in \mathcal{D}} B(E)_{e, e'} (\log B(E)_{e, e'})^2 + 2 \sum_{k \neq 1} \frac{|\langle 1 | G(E) | k \rangle|^2}{1 - \nu_k} , \quad (15)$$

where the $D \times D$ matrix $G(E)$ is defined as $G(E)_{e'e} := B(E)_{e,e'} \log B(E)_{e,e'}$. The detailed derivation and discussion of the variance is deferred to a forthcoming publication [38].

More detailed information is obtained by the *local* Lyapunov exponents which measure the spread of trajectories at a directed edge e or a vertex v :

$$\langle \Lambda_e(E) \rangle = - \sum_{e':o(e')=\tau(e)} B_{e'e} \log B_{e'e} \quad \text{and} \quad \langle \Lambda_v(E) \rangle = \frac{1}{d_v} \sum_{e:\tau(e)=v} \langle \Lambda_e(E) \rangle, \quad (16)$$

where the first sum goes over the set of directed edges starting from the terminus of e and the second sum is over the directed edges terminating at the vertex v .

When considering matrices which correspond to bipartite graphs (e.g., finite trees or linear graphs as associated with tridiagonal matrices) the matrix $B(E)$ is ergodic but not mixing since -1 is in the spectrum. To restore the stronger property of mixing, one uses the fact that the underlying $U(E)$ matrix can be decomposed to four square blocks each of dimension $D/2$, with vanishing two diagonal blocks and unitary off-diagonal blocks denoted by $U_u(E)$ and $U_d(E)$. The spectral secular equation reads $\det(\mathbb{I} - U_u(E)U_d(E)) = 0$. The unitary matrix $\tilde{U}(E) = U_u(E)U_d(E)$ can be used to define a bistochastic matrix \tilde{B} which has the eigenvalue -1 removed. We will use this below for the example of the tridiagonal $G\beta E$ ensemble.

The Lyapunov exponents obey the inequalities

$$0 \leq \langle \Lambda_e(E) \rangle \leq \log d_{\tau(e)} \quad \text{and} \quad 0 \leq \langle \Lambda_v(E) \rangle \leq \log d_v \quad \Rightarrow \quad 0 \leq \langle \Lambda(E) \rangle \leq \frac{1}{D} \sum_{v=1}^V d_v \log d_v. \quad (17)$$

the first two are for the local and the last for the full Lyapunov exponents. The bounds are expressed in terms of the degrees $d_{\tau(e)}$ and d_v of the vertices $\tau(e)$ and v . The lower bounds are obtained if there is one directed edge that follows with probability one, while the maximum is achieved when all connected directed edges can be reached with the same probability $1/d_{\tau(e)/v}$.

The above upper bounds hold for arbitrary bi-stochastic matrices that obey the connectivity of the underlying graph. Typical values for the bi-stochastic matrix $B(E)$ are smaller. If the energy E is chosen outside the spectrum of H then (4) implies $\langle \Lambda(E) \rangle = O\left(\frac{\log E}{E^2}\right)$ in the limit $E \rightarrow \pm\infty$. The same applies to local Lyapunov exponents.

III. INSTRUCTIVE EXAMPLES

The following examples illustrate the application of the the local and global Lyapunov exponents in a few cases, and in particular demonstrate their use for quantifying the underlying chaos.

Adjacency matrices of d -regular graphs

The Lyapunov exponent takes a very simple form if H is equal to the adjacency matrix of a connected d -regular graph. All the vertex scattering matrices $\sigma^{(v)}$ are then identical and the Gershgorin radius is $\Gamma_v = d$ for all vertices. At any given vertex, the transmission and reflection probabilities are $p_t = 4/(E^2 + d^2)$ and $p_r = 1 - (d-1)p_t$. The mean and local Lyapunov exponents are identical - $\langle \Lambda(E) \rangle = -p_r \log p_r - (d-1)p_t \log p_t$ (see Fig. 1). For $d \leq 4$ the maximal Lyapunov exponent is attained at $E = \pm\sqrt{d(4-d)}$ and given by the upper bound $\log d$ derived before in (17). Otherwise the maximal Lyapunov exponent occurs at $E = 0$ where

$$\langle \Lambda(0) \rangle = \frac{2(d-2)^2}{d^2} \log\left(\frac{d}{d-2}\right) + \frac{8(d-1)}{d^2} \log\left(\frac{d}{2}\right). \quad (18)$$

For $d > 4$ this is strictly smaller than the upper bound $\log d$. For $d \rightarrow \infty$ one has $\langle \Lambda(0) \rangle \sim \frac{8 \log(d)}{d} \ll \log d$. These maximal values may be used as benchmarks for local and global Lyapunov exponents in general. One should then replace d by the mean degree of the graph and any degree of non-uniformity decreases the Lyapunov exponent further. It also shows that comparing actual values of Lyapunov exponents on different graph structures needs to be performed with care. It is also worth mentioning that the independence of the local and the mean Lyapunov exponent on V or the detailed graph connectivity does not persist to the variances [38].

A spin-graph Hamiltonian

This example shows how the combination of the local and global Lyapunov exponents provides a tool for analysing the dynamics under study. Consider V_{spin} spins $\sigma^{(v)}$ attached to vertices on a graph that interact pairwise according

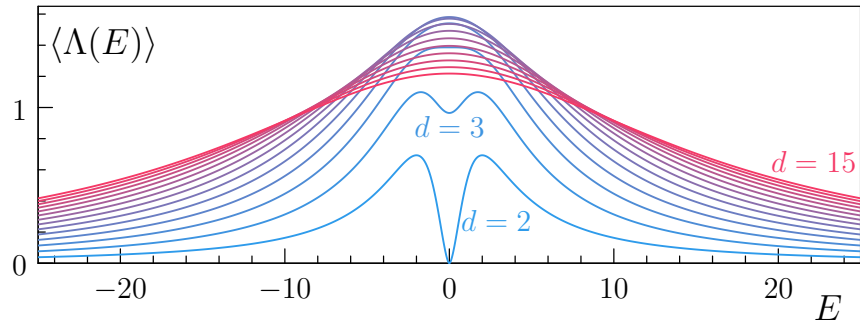


FIG. 1. Mean (or, equivalently, local) Lyapunov exponent for $H = A$ on a d -regular graph as a function of E .

to the connectivity of the graph with real coupling strengths $J_{vw} = J_{wv}$. The Hilbert space of dimension $V = 2^{V_{\text{spin}}}$ is spanned by product states with $\sigma_z^{(v)}$ eigenvalues equal to ± 1 . All spins are subject to a homogeneous magnetic field. For definiteness we choose a Hamiltonian

$$H = \frac{1}{1+\alpha} H_0 + \frac{\alpha}{1+\alpha} H_I, \quad \text{where} \quad (19)$$

$$H_0 = \sum_v \sigma_z^{(v)}, \quad \text{and} \quad H_I = \sum_{v < w} J_{vw} (\sigma_x^{(v)} \sigma_x^{(w)} + \sigma_y^{(v)} \sigma_y^{(w)} + \sigma_x^{(v)} \sigma_z^{(w)} + \sigma_z^{(v)} \sigma_x^{(w)})$$

and $\alpha > 0$ controls the relative strength. In Fig. 2 we show the mean and local Lyapunov exponents for a particular choice of the spin graph and some values of the interaction strength α . The figure shows that the mean Lyapunov exponent remains much smaller than the maximal local one for a weak coupling where eigenstates remain mainly within a subspace of constant $\langle \sum_v \sigma_z^{(v)} \rangle$ while stronger couplings lead to more uniform distributions.

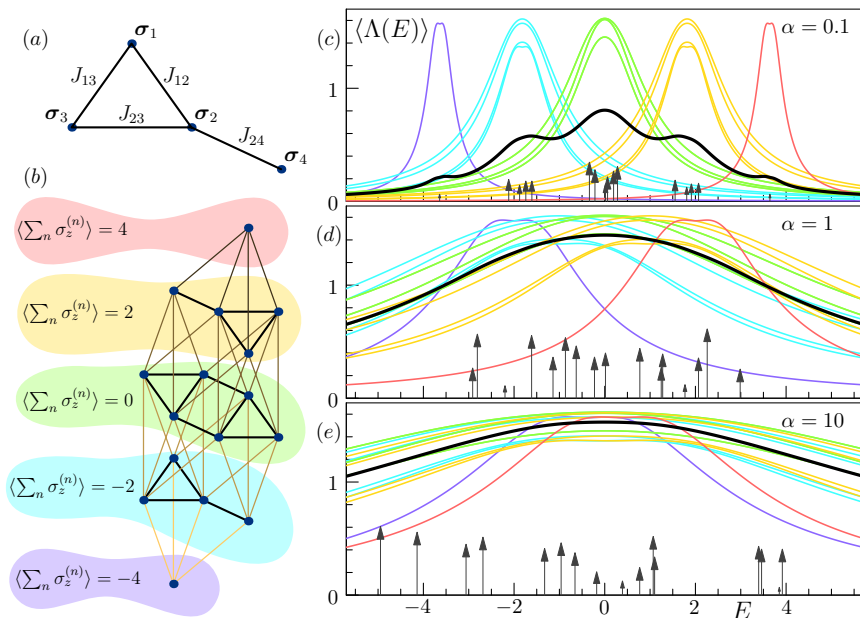


FIG. 2. (a) Spin graph with $V_{\text{spin}} = 4$ vertices.

(b) Corresponding graph of the Hamiltonian where the 16 vertices correspond to spin configurations.

(c-e) Mean Lyapunov exponent (black), local Lyapunov exponents (coloured lines, colours correspond to the ones used in (b)). The spectrum is located at the black arrows where the height corresponds to the participation ratio divided by $V = 16$. We show results for $J_{12} = \frac{1}{3}$, $J_{13} = \frac{\sqrt{5}}{3}$, $J_{23} = \frac{\sqrt{11}}{3}$, and $J_{24} = \frac{1}{\sqrt{3}}$.

The $G\beta E$ ensemble of tridiagonal matrices

The $G\beta E$ ensemble [21] of $V \times V$ tridiagonal matrices offers a simple case for studying the local Lyapunov exponent when the Hamiltonian consists of independently distributed random entries. The diagonal $H_{nn} = a_n$ are distributed normally with zero mean and variance 1. The off-diagonal elements $H_{n-1,n} = H_{n,n-1} = b_n$ are distributed with $p(b_n) = \frac{2}{\Gamma(\frac{\beta n}{2})} b_n^{\beta n - 1} \exp[-b_n^2]$. $\beta > 0$ is a parameter which characterise the ensemble. The spectral statistics coincides with the counterpart Wigner-Dyson ensembles for $\beta = 1, 2, 4$. For large n one finds to leading order

$$\langle b_n \rangle \sim \sqrt{\frac{\beta n}{2}} \left(1 - \frac{1}{4\beta n}\right) \quad \text{and} \quad \langle (b_n - \langle b_n \rangle)^2 \rangle \sim \frac{1}{4}. \quad (20)$$

While the mean of b_n is growing as $\sqrt{\beta n}$, its variance tends to a constant. Hence, by increasing β , the mean value of the off-diagonal entries become increasingly dominant, and the effect of fluctuations diminish. This leads to the mean field discrete Schrödinger equation

$$\sqrt{\frac{\beta}{2}} \left((n-1)^{\frac{1}{2}} \phi_{n-1} + n^{\frac{1}{2}} \phi_{n+1} \right) = E \phi_n \quad (21)$$

with $\phi_0 = \phi_{N+1} = 0$. For $g(n) = n^{\frac{1}{2}} \phi_n$ the ODE analogue of (21) reads

$$-\frac{d^2 g(n)}{dn^2} + \sqrt{\frac{2}{\beta n}} E g(n) = 2g(n). \quad (22)$$

It describes a particle with “energy” 2 subject to a potential $W_{\text{eff}} = \sqrt{\frac{2}{\beta n}} E$, with classical turning point at $n_t = \frac{E^2}{2\beta}$. Fig. 3(a-b) show the absolute square values of the eigenfunctions and the Lyapunov exponents for (21) for two eigenvalues E which belong to the higher (left) and lower (right) parts of the spectrum. The main feature is the appearance of domains on the n axis where the eigenvector amplitudes are small. The domains starts at $n = 1$ and extend up to the classical turning point n_t . This is the classically forbidden domain. The local Lyapunov exponents follow this behaviour, indicating that the phenomenon is captured by the underlying classical dynamics. This feature was studying in detail in [39].

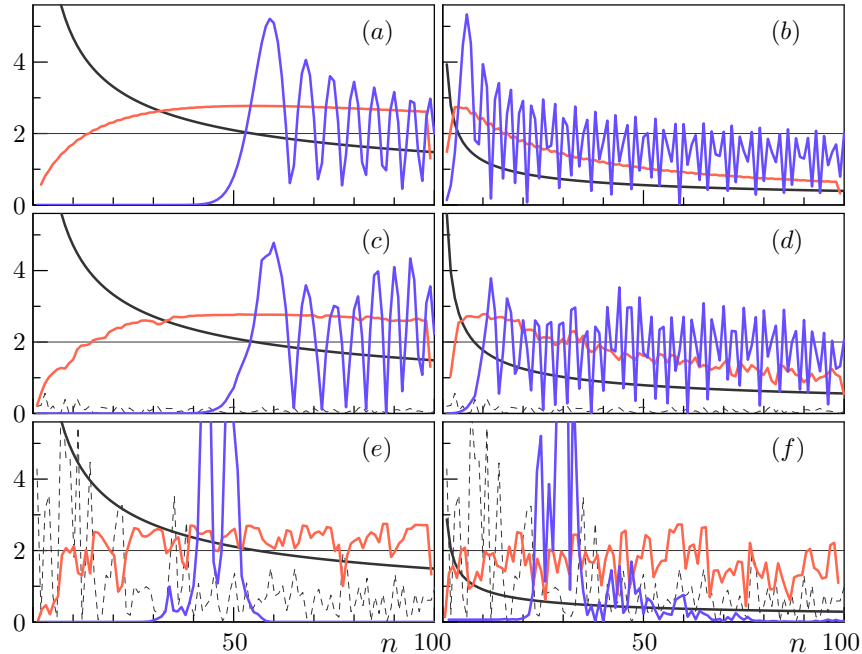


FIG. 3. Squared wavefunctions (Blue, arbitrary scale), local Lyapunov exponents (Red, arbitrary scale), and effective potential $W_{\text{eff}}(n)$ (Black). (a-b) Mean field behaviour for a high (a) and low (b) value of the energy E within the spectrum. (c-d) Single realisation at $\beta = 10$ (the dashed line gives the random potential). (e-f) The same for $\beta = 0.1$.

Fig. 3(c-f) show results for individual realisations of the ensemble for comparison. Fig 3 (c-d) are computed for $\beta = 10$. The wave functions and the local Lyapunov exponents are rather similar to their counterpart shown in

Fig. 3(a-b), albeit more noisy. Fig 3 (e-f) are computed for $\beta = 0.1$. It displays a radically different behaviour because for low values of β the random potential dominates leading to localisation of the wave functions. Note that the dependence on β is through its square root, so the actual effect of changing β is only a factor 10. Averaging over many realisations the Lyapunov exponents approach the results obtained for the mean potentials. Thus, as long as the classical effects dominates in determining the dynamics, the local Lyapunov exponents follow the behaviour of the eigenvectors. It fails when interference dominates and in particular when localisation is not due to the presence of classically forbidden domains.

IV. DISCUSSION AND OUTLOOK

Two issues will be briefly addressed: **(a)** the connection between the present approach and the LR bound and the OTOC; **(b)** a short list of subjects that should be further addressed and open problems.

(a) Both the LR and the OTOC methods use the time dependent commutator $[A(t), B]$, where $A(t) \equiv e^{-\frac{i}{\hbar}Ht} A e^{\frac{i}{\hbar}Ht}$ and B are Hermitian operators selected for the purpose. They show that the norm of the commutator increases (at most) exponentially under some conditions and the exponential growth rate is the indicator of the rate of scrambling induced by H . In the discrete time setting used here we replace the continuous time propagator by $U^t(E)$ and for the sake of clarity we use $A = |a\rangle\langle a|$ and $B = |b\rangle\langle b|$ which project on two directed edges a distance L apart. Choosing the Frobenius operator norm, and abbreviating $U(E)$ by U one obtains after some simple computation

$$\frac{1}{D} \text{tr} \left([U^t A U^{t\dagger}, B] [U^t A U^{t\dagger}, B]^\dagger \right) = \frac{2}{D} (|(U^t)_{ba}|^2 - |(U^t)_{ba}|^4). \quad (23)$$

Denoting by ξ_t the trajectories (9) connecting the edges a and b by traversing t connected edges, and the set of these trajectories by Ξ_t (the number of trajectories is denoted by $|\Xi_t|$) we get for $t \geq L$

$$0 \leq |U_{ba}^t|^2 = \left| \sum_{\xi \in \Xi_t} \prod_{i=1}^{t+1} U_{e_i e_{i-1}} \right|^2 = \sum_{\xi \in \Xi_t} \prod_{i=1}^{t+1} B_{e_i e_{i-1}} + \sum_{\xi \neq \xi' \in \Xi_t} \prod_{i=1}^{t+1} U_{e_i e_{i-1}} \prod_{i'=1}^{t+1} U_{e_{i'} e_{i'-1}} \leq 1. \quad (24)$$

For $L < t < D$ the last sum consists of highly oscillatory terms and therefore can be neglected under appropriate averaging, e.g. with respect to a time window. (It cannot be neglected for t close to D or larger because of the occurrence of increasingly larger number of trajectories which visit the same edges in different orders and therefore have exactly the same phases. This double sum then keeps the expression bounded by 1.) The term $|(U^t)_{ba}|^4$ in (23) can also safely be neglected. Using the fact that the geometric mean is always smaller than the arithmetic mean, one gets

$$|\log[|U_{ba}^t|^2]| \leq t \left\{ \frac{1}{|\Xi_t|} \sum_{\xi \in \Xi_t} \frac{1}{t} \sum_{i=1}^{t+1} |\log[B_{e_i e_{i-1}}]| \right\} - \log[|\Xi_t|] \quad (25)$$

The curly sum appearing in (25) is the analogue of the equation defining the the mean Lyapunov exponent (14), the only difference being that the averaging is different. In the present case all trajectories are treated with equal probability where as in (14) the probabilities of the trajectories are used as weights.

The main advantages of the present formalism is that it allows the computation of the variance of the Lyapunov exponent, and that the trajectories are assigned with an energy E . Practically, the computation of the mean Lyapunov exponent does not require the spectrum or any matrix inversion.

(b) The open problem which are left for forth coming paper [38] are to test the method on systems which are closer to the field where OTOC is applied. It also crucial to investigate to what extent the Lyapunov exponent depends on the spectral parameters of the stochastic matrix, and in particular on the gap between the leading value 1 and the rest. Several of the approximation which were made in the first paragraph above should be better studied, and some scale by which one could compare the Lyapunov exponents of different systems should be established.

ACKNOWLEDGMENTS

We are indebted to Omri Sarig for clarifying several issues in ergodic theory and to Sasha Odin for discussing some of his new results on the $G\beta E$ model before publication, to Hans Weidenmüller who recommended corrections to an early draft of the manuscript, to Holger Schanz and Gregor Tanner for their comments on a later draft, to Micha

Berkooz for discussing the relation to the OTOC approach, and to Tomas Maciażek and to Yiyang Jia for sharing with us their many spins models.

-
- [1] P. Hayden, J. Preskill, *Black holes as mirrors: Quantum information in random subsystems*, J. High Energy Phys. **2007**, 120 (2007).
- [2] Y. Sekino, L. Susskind, *Fast scramblers*, J. High Energy Phys. **2008**, 65 (2008).
- [3] S.H. Shenker, D. Stanford, *Black holes and the butterfly effect*, JHEP **3**, 067 (2014).
- [4] J. Maldacena, S.H. Shenker, D. Stanford, *A bound on chaos*, JHEP **8**, 106 (2016).
- [5] A. Kitaev, *A simple model of quantum holography*, talk given at KITP Program: Entanglement in Strongly-Correlated Quantum Matter, Vol. 7 (USA April, 2015).
- [6] R.J. Garcia, K. Bu, A. Jaffe, *Resource theory of quantum scrambling*, PNAS **120**, e2217031120 (2023).
- [7] K.A. Landsman, C. Figgatt, T. Schuster, N.M. Linke, B. Yoshida, N.Y. Yao, C. Monroe, *Verified quantum information scrambling*, Nature **567**, 61 (2019).
- [8] X. Mi *et al*, *Information scrambling in quantum circuits*, Science **374**, 1479 (2021).
- [9] J. Harris, B. Yan, N.A. Sinitsyn, *Benchmarking Information Scrambling*, Phys. Rev. Lett. **129**, 050602 (2022).
- [10] E.H. Lieb, D.W. Robinson, *The finite group velocity of quantum spin systems*, Commun. Math. Phys. **28**, 251 (1972).
- [11] C.-F. Chen, A. Lucas, C. Yin, *Speed limits and locality in many-body quantum dynamics* Rep. Prog. Phys. **86**, 116001 (2023).
- [12] A. Larkin, Y.N. Ovchinnikov, *Quasiclassical method in the theory of superconductivity*, JETP **28**, 960 (1969).
- [13] I. García-Mata, R.A. Jalabert, D.A. Wisniacki, *Out-of-time-order correlations and quantum chaos*, Scholarpedia **18**, 55237 (2023).
- [14] P. Cvitanović, R. Artuso, R. Mainieri, G. Tanner, G. Vattay, *Chaos: Classical and Quantum*, ChaosBook.org (Niels Bohr Institute, Copenhagen 2020).
- [15] E. Ott, *Chaos in Dynamical Systems* (2nd ed, Cambridge University Press, 2002).
- [16] K. Hashimoto, K.-B. Huh, K.-Y. Kim, R. Watanabe, *Exponential growth of out-of-time-order correlator without chaos: the inverted harmonic oscillator*, JHEP **11**, 068 (2020).
- [17] A. Bhattacharyya, W. Chemissany, S.S. Haque, J. Murugan, B. Yan, *The multi-faceted inverted harmonic oscillator: Chaos and complexity*, SciPost Physics Core **4**, 002 (2021).
- [18] M. Gutzwiller *Chaos in Classical and Quantum Mechanics* (Springer, 1990).
- [19] F. Haake, S. Gnutzmann, M. Kuś, *Quantum Signatures of Chaos*, (4th ed, Springer, 2018).
- [20] O. Bohigas, M.J. Giannoni, C. Schmit, *Characterization of chaotic quantum spectra and universality of level fluctuation laws*, Phys. Rev. Lett. **52**, 1 (1984).
- [21] I. Dumitriu, A. Edelman, *Matrix models for beta ensembles*, J. Math. Phys. **43**, 5830 (2002).
- [22] A.I. Shnirelman, *Ergodic properties of eigenfunctions* [in russian], Uspekhi Mat. Nauk. **29**, 181 (1974).
- [23] Y. Breuer, P. Forrester, U. Smilansky, *Random discrete Schrödinger operators from random matrix theory*, J. Phys A **40**, F161 (2007).
- [24] U. Smilansky, *Quantum chaos on discrete graphs*, J. Phys. A **40**, F621 (2007).
- [25] S. Gnutzmann, U. Smilansky, *Trace formulas for general hermitian matrices*, J. Phys. A **53**, 035201 (2020).
- [26] T. Kottos, U. Smilansky, *Quantum Chaos on Graphs*, Phys. Rev. Lett. **79**, 4794 (1997).
- [27] T. Kottos, U. Smilansky, *Periodic Orbit Theory and Spectral Statistics for Quantum Graphs*, Annals of Physics **274**, 76 (1999).
- [28] S. Gnutzmann, U. Smilansky, *Quantum graphs and their applications to quantum chaos and universal spectral statistics*, Advances in Physics **55**, 527 (2006).
- [29] F. Barra, P. Gaspard, *Classical Dynamics on Graphs*, Phys. Rev. E **63**, 066215 (2001).
- [30] G. Berkolaiko, *Spectral gap of doubly stochastic matrices generated from equidistributed unitary matrices*, **34**, L319 (2001).
- [31] G. Tanner, *Unitary-stochastic matrix ensembles and spectral statistics* J. Phys. A **34**, 8485 (2001).
- [32] P. Pakonski, K. Życzkowski, M. Kuś, *Classical 1D maps, quantum graphs and ensembles of unitary matrices*, J. Phys. A **34**, 9303 (2001).
- [33] S. Gnutzmann, A. Altland, *Universal Spectral Statistics in Quantum Graphs*, Phys. Rev. Lett. **93**, 194101 (2004).
- [34] S. Gerschgorin, *Über die Abgrenzung der Eigenwerte einer Matrix* [in german], Izv. Akad. Nauk. USSR Otd. Fiz.-Mat. Nauk **6**, 749–754 (1931).
- [35] P. Walters, *An Introduction to Ergodic Theory* (Springer, New York, 1982).
- [36] W. Parry, M. Pollicott, *Zeta Functions and the Periodic Orbit Structure of Hyperbolic Dynamics*, (Société Mathématique de France, 1990).
- [37] Omri Sarig, *Lecture notes on Ergodic Theory*, Weizmann Institute (2023), <https://www.weizmann.ac.il/math/sarigo/lecture-notes>.
- [38] Sven Gnutzmann and Uzy Smilansky, To be published.
- [39] S. Sodin, O. Zeitouni, *On the shape of the eigenvectors of tridiagonal $G\beta E$ matrices*, to be published.